Magnetic Field Dependence of Electron Spin Polarization Generated through Radical−Triplet Interactions

Eli Stavitski, Linn Wagnert, and Haim Levanon*

Department of Physical Chemistry and Farkas Center for Light-Induced Processes, The Hebrew University of Jerusalem, Jerusalem 91904, Israel

Received: November 5, 2004; In Final Form: December 2, 2004

The magnetic field dependence of electron spin polarization (ESP), generated in free radicals when they encounter photoexcited triplets, was measured experimentally and analyzed theoretically. The time-resolved electron paramagnetic resonance measurements were performed with a microwave setup consisting of low-loss dielectric ring resonators with tunable microwave frequencies and the corresponding magnetic fields. The ESP of the radical was found in the magnetic field range of 170−370 mT, and the results of the calculation based on the numerical solution of the stochastic Liouville equation were found to be in line with the experimental data showing that ESP decreases when the magnetic field increases.

1. Introduction

Electron spin polarization (ESP), i.e., the non-Boltzmann population of the electron spin levels, is generated in a variety of photochemical and photophysical reactions.[1,2] The interaction of free radicals with photoexcited triplets in solution resulting in highly spin-polarized radicals[3−7] is one of those processes. The classical mechanisms of chemically induced dynamic electron polarization (CIDEP), i.e., the triplet mechanism and the radical pair mechanism, fail to account for this phenomenon.[8] Thus, two complementary mechanisms contributing to ESP generation were invoked, namely, electron spin polarization transfer (ESPT) and radical−triplet polarization mechanism (RTPM).[8] The former is attributed to the interaction of free radicals with spin-polarized triplets, while in the latter mechanism polarization of the triplet prior to the encounter is not required. It is evident that the properties of the radical, triplet, and solvent determine the magnitude of the resulting ESP. Specifically, the molecular dimensions and the solvent viscosity, which affect the mutual diffusion of the interacting species, should be taken into account. One should also consider the magnetic properties of the radicals and triplets, such as the line widths of the EPR spectra, the triplet zero-field splitting (ZFS) parameter, and the spin−lattice relaxation (SLR) times of the radicals and the triplets.

In a recent study, a comprehensive theoretical treatment of ESPT and RTPM phenomena taking into account all of the above-mentioned parameters was developed.[9] Beyond the basic aspects of ESP generated during the radical−triplet (R−T) encounters, this phenomenon may lead to practical applications in microwave (MW) technology.[10] Such applications are based on the fact that the macroscopic magnetic permeability of the chemical system can be directly related to photoinduced ESP via the change in the real (leading to a phase shift) or imaginary parts (leading to an amplification/attenuation) of permeability providing a platform for MW devices with very low noise characteristics even at room temperature.[10] To approach this goal, the high ESP requirement should be accompanied by the specially designed MW resonators.[11,12] The relevant resonator should possess high filling and quality factors (η and Q, respectively) and be sufficiently small to allow efficient photoexcitation of the chromophore in the sample.

In addition to the above-mentioned parameters affecting the ESP magnitude, one should also consider the magnetic field strength. As shown in previous studies, ESP in the R−T encounter is generated mainly in the crossing points of the quartet−doublet energy levels that are formed upon the R−T interaction. As a consequence, the magnetic field should determine the R−T distance at which the level crossing occurs (Figure 1). A qualitative prediction about the effect of the magnetic field on the magnitude of ESP has been reported,[13] showing that the magnitude of ESP is expected to decrease when the magnetic field increases. Preliminary time-resolved electron paramagnetic resonance (TREPR) experiments at the X- (10 GHz) and D-bands (130 GHz) provided confirmation of the theoretical prediction.[14] Nevertheless, it was difficult to analyze the results quantitatively, since we could not compare different types of resonators operating at two MW frequencies. The same type of resonators with a single variable, i.e., the magnetic field strength, must be used to overcome this difficulty and make the comparison on a quantitative basis.

In this work, we have employed low-loss dielectric resonators and varied the resonance frequency and corresponding magnetic field by changing the resonator dimensions. Here, we present the experimental results at the X- (∼10 GHz) and S-bands (∼5 GHz) as well as theoretical calculations based on recent extensive theoretical papers.[9,13]

2. Experimental Section

Chemical System. The free-base etioporphyrin I (Frontier Scientific), the deuterated modification of the trityl radical (Nycomed Innovations, U.S. Patent 6,013,810), and the solvents were used without further purification (Figure 2). The solvent (viscosity ∼30 cP) was prepared by mixing 10% cyclohexanone (to increase the solubility of the trytil radical), 20% chloronaphthalene, and 70% heavy paraffin oil (Sigma-Aldrich). The porphyrin and radical concentrations were ∼2 mM. The solution was degassed in a 1.2 mm o.d. Pyrex tube by several freeze−pump−thaw cycles and sealed under vacuum.

10.1021/jp044937o CCC: $30.25
Published on Web 01/25/2005

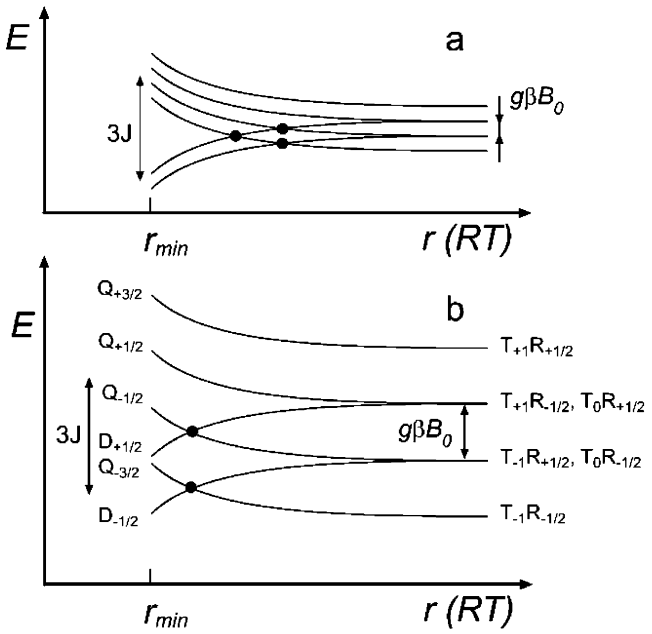

Figure 1. Schematic description of the energy levels of the radical−triplet (R−T) pair. T and R are the states of the separated triplet and radical, the Q and D states are the quartet and doublet states, formed upon R−T interaction, respectively, and r_{min} is the shortest distance of approach, defined by the molecular radii. Two cases are discussed: (a) Exchange interaction J is larger than the Zeeman energy, $g\beta B_0$, where the level crossing is easily attained resulting in effective radical ESP, and (b) J is smaller than $g\beta B_0$ where the level crossing between $D_{+1/2}$ and $Q_{-3/2}$ cannot be achieved.

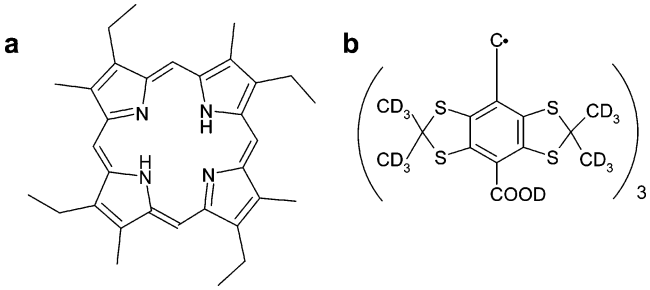

Figure 2. Chemical structure of etioporphyrin I (a) and deuterated trytil radical (b).

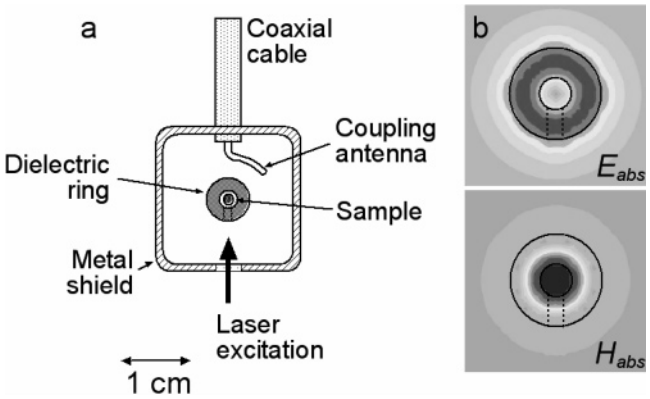

Figure 3. (a) Schematic layout of the resonator based on a high-permittivity dielectric ring. (b) Calculated electric and magnetic field distribution for the dielectric resonator.

Measurements. A home-built network analyzer coupled with a laser source was used to measure the photoinduced ESP effect. The MW signal generator (Wiltron 6638A) was connected to the MW resonator via a circulator, and the radiation reflected from the resonator was measured by an HP 8472B crystal detector. The signal, amplified by a broad-band video amplifier, was transferred to the oscilloscope which is triggered by a photodiode. MW power was kept at ~1 mW to prevent saturation of the sample. The sample was illuminated by a small diameter laser beam (Lightware Nd:YAG laser, second harmonics, 532 nm) with a repetition rate of 6 Hz. Optical absorption measurements indicate that, unlike etioporphyrin, the trityl radical does not absorb at 532 nm. The varying magnetic field was produced with a Walker HV-7H electromagnet.

The resonator used in this study is a ring dielectric resonator, made of low-loss ceramics. The schematic layout of the resonator is given in Figure 3a. The operational frequency of this structure may be calculated, approximately, by the following equation:[15]

$$f_{\mathrm{GHz}} = \frac{34}{a\sqrt{\epsilon}}\left(\frac{a}{h} + 3.45\right) \qquad (1)$$

where ϵ is the dielectric constant of the material, a is the radius of the dielectric ring (in millimeters), and h is its height. In this study, two ceramic materials with ϵ values of ~41 and ~32 were used (TransTech Inc. 4500 and 8700 series). For both materials, two different sizes of rings were used (h/a = 2.6 mm/3.0 mm and h/a = 4.6 mm/5.2 mm). The dimensions and dielectric constants of the rings cover the range of frequencies between 4 and 11 GHz (which corresponds to magnetic fields of 170−370 mT). A hole ($d \approx 1.2$ mm) was drilled in the resonator to allow the sample to be photoexcited. The dielectric ring was placed into a hollow brass structure, functioning as a Faraday cage, to prevent radiation losses from the resonator. The coupling to the microwave circuit was achieved by means of an antenna made of the central conductor of a semirigid coaxial cable (Figure 3a). Since the antenna is perpendicular to the resonators's cylindrical axis (out-of-plane), the fundamental $T_{01\delta}$ mode could be excited (Figure 3b). The distance between the antenna and the ring was matched to achieve critical coupling. The calculations of the electromagnetic (EM) fields distribution were performed with the CST Microwave Studio computer program package (CST GmbH).[16]

3. Results and Discussion

The EPR signal intensity, i.e., MW absorption/emission by a paramagnetic sample, in the resonator is given by (under nonsaturating conditions)[17]

$$\text{EPR signal intensity} \propto \eta Q\sqrt{N_{\mathrm{MW}}}P \qquad (2)$$

where P is the relative population difference of the Zeeman levels, i.e., polarization, and N_{MW} is the applied MW power. Thus, the TREPR results from an R−T system (Figure 2) in which the known characteristics of the resonators leave the system with only one variable, i.e., the magnetic field, allow us to unambiguously determine the effect of the variable on photogenerated ESP.

The Q factors of the resonators with the sample were measured by sweeping the MW frequency over the resonance dip and were found to be in the range of 1400−2000, depending on the size and properties of the dielectric rings. To calculate η, which reflects the strength of the microwave magnetic field (H_1) at the chemical sample, one should know the EM field

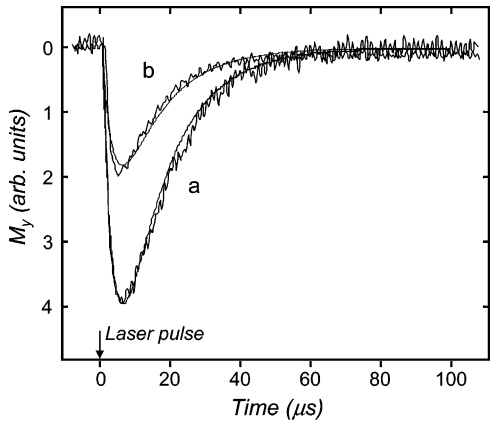

Figure 4. Temporal behavior of the radical magnetization. The TREPR signals are shown for the case of $B_0 = 180$ (a) and 370 mT (b) along with the calculated time profiles (smooth lines). The parameters used for the calculation are as follows: $J = 3 \times 10^{11}$ rad/s and $\alpha = 2.5$ Å^{-1}, $r_R = r_T = 5$ Å, $D = 8 \times 10^9$ rad/s, initial triplet concentration = 0.5 mM, and $T_1^R \approx 20$ μs.[22] Experimental curves were normalized with filling and quality factors of the specific resonators used for different magnetic fields.

distribution in the cavity.[17]

$$\eta = \frac{\int_{\text{sample}} H_1^2 \, dV}{\int_{\text{resonator}} H_1^2 \, dV} \tag{3}$$

Since we are concerned with light-induced experiments, the integration of the numerator should be performed only over the illuminated part of the sample. For the disc-shaped dielectric resonators, an analytical solution for the field distribution does not exist.[18] Instead, one may use simple approximate models[19] or a numerical procedure based on the finite-element method.[20] We have chosen the latter approach, which also takes into account the distance of the dielectric ring from the metal walls of the shield. The calculated electric and magnetic field distributions in the resonator are depicted in Figure 3b. Taking into account that the i.d. of the tube is 0.6 mm and the diameter of the laser spot is ~1.2 mm and assuming that the sample insertion does not vary the field distribution significantly, η was calculated to be $\sim 6 \times 10^{-2}$ and $\sim 1.4 \times 10^{-2}$ for ring radii of 3 and 5.2 mm, respectively.

Temporal evolution of photoinduced M_y magnetization at two MW frequencies (5.2 and 10.6 GHz) is shown in Figure 4. The emissive signals are associated with radical ESP, generated via the R−T encounters, and their decay is due to the radical SLR.[7,9,21] The amplitude of the signal was found to depend on B_0, while the temporal behavior was unchanged over the entire B_0 range. It should be noted that for each B_0 value the Q and η of the resonators employed were different. Therefore, to obtain consistent results, the kinetic curves were normalized with the specific Q and η for each case.

To quantitatively correlate the experimental results with the theory, we have treated the spin dynamics of the R−T pair in terms of the stochastic Liouville equation (SLE) in which the effects of spin interactions and relative molecular diffusion are considered.[9,21,23,24]

$$\frac{\partial r\boldsymbol{\rho}(r,t)}{\partial t} = D_r \frac{\partial^2 r\boldsymbol{\rho}(r,t)}{\partial r^2} - i[\boldsymbol{H}, r\boldsymbol{\rho}(r,t)] \tag{4}$$

Here $\rho(r,t)$ is the density matrix of the R−T pair at time t and distance r, and D_r is a diffusion coefficient for the relative motion of the radical and triplet molecules. $\boldsymbol{H}$ is the spin Hamiltonian of the triplet−radical pair given by[9,25]

$$\boldsymbol{H} = \boldsymbol{H}_Z + \boldsymbol{H}_{ZFS} + \boldsymbol{H}_{EX} \tag{5}$$

$\boldsymbol{H}_Z$ is the Zeeman part, assuming the g-factors of the radical and triplet are the same

$$\boldsymbol{H}_z = g\beta B_0(\boldsymbol{S}_R + \boldsymbol{S}_T) \tag{6}$$

$\boldsymbol{S}_R$ and the $\boldsymbol{S}_T$ are the spin operators of the radical and triplet, respectively, and the ZFS Hamiltonian of the photoexcited triplet, $\boldsymbol{H}_{ZFS}$ is

$$\boldsymbol{H}_{ZFS} = D\left(\boldsymbol{S}_z^2 - \frac{1}{3}\boldsymbol{S}^2\right) + E(\boldsymbol{S}_x^2 - \boldsymbol{S}_y^2) \tag{7}$$

where D and E are the ZFS parameters and x, y, and z are the principal axes of the ZFS interaction. For free-base etioporphyrin studied here, $D \gg E$, and the second term can be neglected. The exchange Hamiltonian is given by

$$\boldsymbol{H}_{EX} = -J(r)(1 + 3\boldsymbol{S}_R\boldsymbol{S}_T) \tag{8}$$

The exchange interaction is expressed by $J(r) = J_0 e^{-\alpha(r-d)}$, where d is the distance of closest approach and α is a free parameter. At large R−T distances the eigenstates of the spin Hamiltonian are reduced to the spin states of noninteracting species, while at short separations the eigenstates coincide with eigenstates of the total spin $\boldsymbol{S} = \boldsymbol{S}_R + \boldsymbol{S}_T$. Thus, for $S = 3/2$, four quartet (Q) states are generated

$$|Q_{\pm 1/2}\rangle = \sqrt{2/3}|T_0\rangle|R_{\pm 1/2}\rangle + \sqrt{1/3}|T_{\pm 1}\rangle|R_{\mp 1/2}\rangle$$
$$|Q_{\pm 3/2}\rangle = |T_{\pm 1}\rangle|R_{\pm 1/2}\rangle \tag{9}$$

and for $S = 1/2$, two excited doublet states (D) are formed

$$|D_{\pm 1/2}\rangle = -\sqrt{1/3}|T_0\rangle|R_{\pm 1/2}\rangle + \sqrt{2/3}|T_{\pm 1}\rangle|R_{\mp 1/2}\rangle \tag{10}$$

These six energy levels are split by the exchange interaction and cross each other at the R−T distance determined by J_0, α, and B_0 (Figure 1). It should be emphasized that the Q−D levels may cross only when $J(r_{min}) > g\beta B_0$, which occurs in X-band and lower frequencies for the chemical systems under study (Figure 1). The fluctuating triplet ZFS interaction induces nonadiabatic quartet−doublet transitions in three points of Q−D level crossing. Such level mixing upon R−T encounter is followed by quenching of the triplet to its ground singlet state, and the triplet−radical separation results in non-Boltzmann spin polarization of the radical.[9,13,24] Taking into account the transition probabilities for each level crossing region, eq 4 can be solved analytically[13,24,26,27] or numerically.[9] The numerical solution is based on the finite difference approach developed earlier.[28] In this approach, eq 4 is first treated by the Laplace transform to avoid the time derivative, and then the interval between the fully separated distance and the distance of closest approach, r_{min}, is divided into finite small distances. This enables us to express the Laplace-transformed SLE with a matrix form, which is convenient to solve. The complete treatment is described elsewhere,[9] where the resulting equations are solved for the X-band case ($B_0 = 340$ mT). Here we employed the same approach to calculate the radical polarization for different magnetic fields, mentioned above (150−400 mT), keeping other relevant parameters constant: (a) $J = 3 \times 10^{11}$ rad/s and $\alpha = 2.5$ Å^{-1}, (b) molecular radii of the radical and triplet molecules $r_R = r_T = 5$ Å, and (c) ZFS parameter $D = 8 \times 10^9$ rad/s as

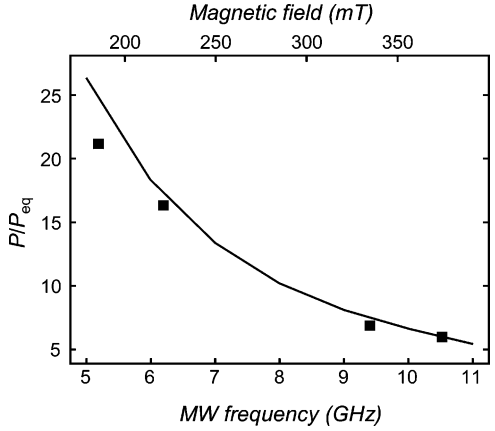

Figure 5. Experimental (dots) and calculated (solid line) radical polarization generated via radical−triplet interaction. The calculation is carried out with the parameters described in the text. Note that the calculated results refer to the ratio between polarization acquired in the R−T encounter and equilibrium polarization, P_{eq}. Since the equilibrium polarization cannot be found quantitatively by using the CW-TREPR method, all experimental results were normalized by a single constant factor to fit the theoretical smooth curve.

determined from the line shape analysis of the TREPR spectrum of the etioporphyrin photoexcited triplet state, taken in the crystalline phase of liquid crystal E-7.[29] With these parameters the numerical calculations result in a polarization magnitude at different magnetic fields, as shown by the smooth line in Figure 5. It clearly shows that the radical polarization depends on the external magnetic field.

To determine the extent to which the experimental results fit the theoretical analysis, described above, the following photochemical reactions associated with the ESP process should be considered:[7]

$$T \xrightarrow{h\nu} {}^{1*}T \xrightarrow{ISC} {}^{3*}T_p \tag{11a}$$

$${}^{3*}T_p + R \xrightarrow{ESPT} R_p + {}^{3*}T_p \tag{11b}$$

$${}^{3*}T_p + R \xrightarrow{RTPM} R_p + 2/3\,{}^{3*}T_p + 1/3T \tag{11c}$$

$${}^{3*}T_p \xrightarrow{quenching} T \tag{11d}$$

T and R in the eqs 11a−d are the triplet and radical species, respectively, and the subscript p stands for the polarized state. In the ESPT mechanism, the radical polarization is generated directly from the triplet (eq 11b). However, inspection of Figure 4 shows that the radical polarization reaches its maximum at ∼8 μs, significantly exceeding the triplet SLR time (∼0.5 μs, in line with the results obtained for other free-base porphyrins[30]). It is conceivable that in the present case ESPT (eq 11b) can be neglected, and only RTPM is considered (eq 11c). For this discussion, eqs 11a,c,d were analyzed in terms of the Bloch equations, modified to account for the chemical kinetics[13,31]

$$\frac{dM_y}{dt} = -\frac{M_y}{T_2^R} + \omega_1 M_z \tag{12a}$$

$$\frac{dM_z}{dt} = -\omega_1 M_y + \frac{P_{eq}[R]' - M_z}{T_1^R} + k_q P[T][R]' \tag{12b}$$

$$\frac{d[T]}{dt} = -k_q[T][R] - 2k_{TT}[T]^2 - k_T[T] \tag{12c}$$

where P_{eq} is the radical polarization in equilibrium and P is the radical polarization generated during the R−T encounters. Radical−triplet and triplet−triplet quenchings and triplet decay rate constants are denoted by k_q, k_{TT}, and k_T, respectively. [T] and [R] are the triplet and radical concentrations, respectively, and in order to account for magnetization units, $[R]' = \beta[R]$ (β is the Bohr magneton). M_y, M_z, T_1^R, and T_2^R are the y- and z-components of the radical magnetization and the SLR and spin−spin relaxation times, respectively. The last term in eq 12b accounts for the radical magnetization acquired through the R−T interaction, and eq 12c describes the decay of the triplet.

To fit the TREPR experimental curves of M_y (Figure 4), the coupled differential equations (12a−c) should be solved. The calculated time profiles are shown in Figure 4 (smooth lines), from which the radical polarization, P, was extracted for each of the four magnetic field values. At this stage, we can compare the results obtained from the theoretical calculation with the experimental results. For each B_0, equilibrium polarization, P_{eq}, can be calculated by the Boltzmann distribution as $P_{eq} = (1 - \exp(-g\beta B_0/kT))/(1 + \exp(-g\beta B_0/kT))$, and the ratio P/P_{eq}, obtained experimentally, is given by the squares in Figure 5. One can see that the experimentally measured RTPM polarization of the radical is in full agreement with the numerical solution of SLE.

In conclusion, we have studied the dependence of the radical spin polarization, generated via the R−T interactions, on the applied magnetic field. This task was accomplished using a microwave setup with specially designed dielectric resonators. The results confirm that ESP is inversely proportional to magnetic field strength. Furthermore, the study of radical−triplet interactions, which generate high ESP, extends beyond its basic aspects suggesting that application of the R−T systems in MW technology may be feasible.[10,32] Therefore, we consider this research not only an additional step to further understanding the processes governing ESP but also a step leading to fulfilling the threshold requirement of a microwave amplifier based on photoexcited "smart" chemical systems.

Acknowledgment. This work is in partial fulfillment of the requirements for a Ph.D. (E.S.) at the Hebrew University of Jerusalem (HUJ). Work at HUJ was supported by the Israel Ministry of Science, the U.S.-Israel BSF, the Israel Science Foundation, and the DFG. The Farkas Research Center is supported by the Bundesministerium für die Forschung und Technologie and the Minerva Gesellschaft für Forchung GmbH, FRG. Valuable discussions with Dr. A. Blank are greatly appreciated. We are thankful to Nycomed Innovations for providing us with the deuterated trytil radical. We are also grateful to Dr. M. C. Thurnauer and Dr. O. Poluektov for carrying out the D-band experiments through our BSF program (H.L. and M. C. Thurnauer).

References and Notes

(1) Muus, L. T.; Atkins, P. W.; McLauchlan, K. A.; Pedersen, J. B. *Chemically Induced Magnetic Polarization*; Reidel: Dordrecht, The Netherlands, 1977.

(2) Salikhov, K. M.; Molin, Y. N.; Sagdeev, R. Z.; Buchachenko, A. L. *Spin Polarization and Magnetic Effects in Radical Reactions*; Elsevier: Amsterdam, 1984.

(3) Thurnauer, M. C.; Meisel, D. *Chem. Phys. Lett.* **1982**, *92*, 343.

(4) Blattler, C.; Jent, F.; Paul, H. *Chem. Phys. Lett.* **1990**, *166*, 375.

(5) Rozenshtein, V.; Zilber, G.; Rabinovitz, M.; Levanon, H. *J. Am. Chem. Soc.* **1993**, *115*, 5193.

(6) Kawai, A.; Obi, K. *Res. Chem. Intermed.* **1993**, *19*, 865.

(7) Blank, A.; Levanon, H. *J. Phys. Chem. A* **2000**, *104*, 794.

(8) Fujisawa, J.; Ohba, Y.; Yamauchi, S. *J. Phys. Chem. A* **1997**, *101*, 434.

(9) Blank, A.; Levanon, H. *Mol. Phys.* **2002**, *100*, 1477.
(10) Blank, A.; Levanon, H. *Appl. Phys. Lett.* **2001**, *79*, 1694.
(11) Yariv, A. *Quantum Electronics*; Wiley: New York, 1967.
(12) Blank, A.; Stavitski, E.; Levanon, H.; Gubaydullin, F. *Rev. Sci. Instrum.* **2003**, *74*, 2853.
(13) Blank, A.; Levanon, H. *J. Phys. Chem. A* **2001**, *105*, 4799.
(14) Stavitski, E.; Levanon, H.; Thurnauer, M. C.; Poluektov, O. Argonne National Laboratory, Argonne, IL. Unpublished results, 2002.
(15) Kaifez, D.; Guillon, P. *Dielectric Resonators*; Noble Publishing: Atlanta, GA, 1998.
(16) See www.cst.de.
(17) Poole, C. P. *Electron Spin Resonance: A Comprehensive Treatise on Experimental Techniques*; Dover: New York, 1997.
(18) Jaworski, M.; Sienkiewicz, A.; Scholes, C. P. *J. Magn. Reson.* **1997**, *124*, 87.
(19) Fiedziuszko, S. J.; Jelenski, A. *IEEE Trans. Microwave Theory Tech.* **1971**, *MTT-19*, 778.
(20) Kajfez, D.; Glisson, A. W.; James, J. *IEEE Trans. Microwave Theory Tech.* **1984**, *32*, 1609.
(21) Kobori, Y.; Takeda, K.; Tsuji, K.; Kawai, A.; Obi, K. *J. Phys. Chem. A* **1998**, *102*, 5160.
(22) SLR time was found by an FT-EPR experiment, using an inversed recovery pulse sequence. Further experimental details of the FT-EPR experiment are given in ref 6.
(23) Goudsmit, G. H.; Paul, H.; Shushin, A. I. *J. Phys. Chem.* **1993**, *97*, 13243.
(24) Shushin, A. I. *Chem. Phys. Lett.* **1993**, *208*, 173.
(25) Kobori, Y.; Kawai, A.; Obi, K. *J. Phys. Chem.* **1994**, *98*, 6425.
(26) Shushin, A. I. *J. Chem. Phys.* **1993**, *99*, 8723.
(27) Adrian, F. J. *Chem. Phys. Lett.* **1994**, *229*, 465.
(28) Freed, J. H.; Pedersen, J. B. *Adv. Magn. Reson.* **1976**, *8*, 1.
(29) Triplet line shape analysis procedure is described in detail in: Gonen, O.; et al. *J. Chem. Phys.* **1986**, *84*, 4132. The description of the experimental setup is given in: Berg, A.; et al. *J. Phys. Chem. A* **1999**, *103*, 8372.
(30) Regev, A.; Levanon, H.; Murai, T.; Sessler, J. L. *J. Chem. Phys.* **1990**, *92*, 4718.
(31) Verma, N. C.; Fessenden, R. W. *J. Chem. Phys.* **1976**, *65*, 2139.
(32) Levanon, H.; Blank, A. U.S. patent 6,515,539, February 4, 2003.